Dissociative Multiple Ionization following Valence, Br(3d), and Si(2p) Inner Shell Photoexcitation of $SiBr_4$ in the Range of 30−133 eV

Bong Hyun Boo,*,† Zhaoyang Liu,† Sang Yeon Lee,‡ and Inosuke Koyano§

Department of Chemistry, Chungnam National University, Taejon 305-764, Korea, and Center for Molecular Science, 373-1 Kusung-dong, Yusung-gu, Taejon 305-701, Korea; Department of Industrial Chemistry, Kyungpook National University, Taegu 702-701, Korea; and Department of Material Science, Himeji Institute of Technology, 1479-1 Kanaji, Kamigohri, Hyogo 678-12, Japan

Received: May 19, 1998

The photoionization of $SiBr_4$ in the valence shell, and the Br(3d) and Si(2p) inner shell excitation/ionization regions, has been studied by using a time-of-flight mass spectrometer and synchrotron radiation over the range 30−133 eV. The photoionization efficiency curve of $SiBr_4$ has been recorded as a function of the incident photon energy. Dissociation processes of $SiBr_4$ have also been investigated by photoelectron−photoion coincidence and photoion-photoion coincidence (PIPICO) techniques. Various monocations of Br_n^+ ($n = 1, 2$) and $SiBr_n^+$ ($n = 0-4$) are detected along with dications of Br^{2+} and $SiBr_n^{2+}$ ($n = 0, 1, 3$) in the energy range. Various dissociation patterns are proposed based on the measurements of the ion time-of-flight differences in the PIPICO mode. The dominant dissociation pattern is found to be Si^+-Br^+ and $SiBr^+-Br^+$ in the whole energy examined. In the Br(3d) excitation region, however, a fragmentation leading to ion pair such as $SiBr_3^+-Br^+$ also plays an important role in the dissociation of the core-excited $SiBr_4$. With the help of ab initio Hartree−Fock and previous CI calculations, we estimate the term values and symmetries of the discrete core-excited states. This study of the specific excitation and dissociation of molecules provides information on energy dissipation processes of the core-excited states.

I. Introduction

Dissociative ionization processes of core−hole excited molecules are of much interest because site selectivity in the fragmentation is observed owing to the large amount of energy stored in a specific atom upon the core excitation. Among various compounds, silicon-containing compounds have drawn much attention owing to the central role of silicon and its compounds in the fabrication of microelectronics components and other high-technology devices.

Energetics, spectroscopy, and dynamics of the core−hole excited states involving core levels of Si(1s),[1−3] Si(2s),[3] and Si(2p)[3−22] have been investigated by various methods such as X-ray photoabsorption spectroscopy,[1−3] the discrete variational (DV) Xα method,[16] multiple-scattering (MS) Xα method,[17] and electron energy loss spectroscopy.[18] All the previous studies of silicon-containing molecules show that the transition of Si-(2p) core electron to the first antibonding orbital occurs when the incident photon energy reached about 103 eV, the value being more or less shifted with different ligands. It is accepted as a universal rule that the chemical shifts of photoelectron and Auger lines are linearly dependent on the average differences in Pauling's electronegativities to the nearest neighbors, $\Delta\bar{\chi}_P$.[23]

Compared to the excitation of Si(2p) core electron, studies of the excitation of Br(3d) core electron are much fewer. In the earliest studies of Br(3d) photoabsorption, three resonances are observed at 64.38, 65.43, and 64.97 eV identified as $^2P_{3/2} \rightarrow {}^2D_{5/2}$, $^2P_{3/2} \rightarrow {}^2D_{3/2}$, and $^2P_{1/2} \rightarrow {}^2D_{3/2}$ transitions, respectively, involving $3d^{10}4s^24p^5 \rightarrow 3d^94s^24p^6$ excitation.[24] Photoelectron spectroscopy on a laser-photodissociated Br gas jet backlit provides positions of 64.54. 65.58, and 65.3 eV.[25] Employing the dual-laser-produced plasma technique, Cummings and O'Sullivan reported the 3d photoabsorption spectra of Br, Br^+, and Br^{2+} in the 60−90 eV region.[26] They observed that 3d → 4p transitions occurred in every case while 3d → *n*p ($n > 4$) features were also obtained in the spectrum of neutral bromine.

Besides the excitation of atomic neutral and ions, Olney et al. have investigated the Br M shell excitation in BrCN molecule using dipole (e,e) spectroscopy in the wide range of 5−451 eV.[27] It is shown that the Br(3d) region of the BrCN photoabsorption spectrum is composed of two regions. The lower region (below 76.5 eV) consists of broad peaks owing to transitions of Br(3d) electron to virtual valence orbitals of BrCN, and the upper region (above 76.5 eV) consists of sharp peaks corresponding the transitions to Rydberg orbitals. Furthermore, they obtained the information on the Coulomb explosion decay channels of doubly and triply charged molecular ions from the photoion−photoion coincidence (PIPICO) measurements in the photon energy region 40−130 eV.[28]

One can characterize the dissociative ionization following the Si(2p) and Br(3d) photoexcitation in molecule $SiBr_4$ and compare the dissociation patterns in the discrete excitation region. It is quite unfortunate that no photoabsorption studies of $SiBr_4$ have been reported in both the Si(2p) and Br(3d) regions. The only contribution to $SiBr_4$ is that Bodeur et al. have reported the photoabsorption spectrum and term values of core-excited states in the Si(1s) region.[1,2]

* To whom correspondence should be addressed. E-mail: BHBoo@Hanbat.chungnam.ac.kr.
† Chungnam National University and Center for Molecular Science.
‡ Kyungpook National University.
§ Himeji Institute of Technology.

10.1021/jp982313a CCC: $15.00
Published on Web 10/02/1998

In this report, we present our recent experimental and theoretical results of the dissociative ionization following valence region, and Si(2p) and Br(3d) regions between 30 and 133 eV. We have assigned the discrete resonances involving the core-to-valence and core-to-Rydberg excited states and elucidated the dissociation patterns in the valence and inner shell excitation/ionization regions.

II. Experimental and Theoretical Section

The time-of-flight (TOF) mass spectrometer is coupled to a constant-deviation grazing incidence monochromator installed at the BL3A2 beam line of the Ultraviolet Synchrotron Orbital Radiation (UVSOR) facility in Okazaki. The principle and construction of the whole apparatus have been described in detail previously.[29,30] One feature of the TOF mass spectrometer is that the length of the field-free tube is adjustable, which facilitates the detection of metastable ions and makes possible to obtain better mass-resolved spectra. In addition, the mass detection angle can be varied by rotating the mass spectrometer in the plane perpendicular to the direction of incident photon beam. For all the experiments in this work, the TOF length and angle were fixed at 40 cm and 55°, the so-called "pseudomagic angle",[31,32] respectively.

For these mass spectrometric studies, two operating modes, photoelectron−photoion coincidence (PEPICO) and photoion−photoion coincidence (PIPICO), are utilized. The main difference between the two modes is that the different charged species are sampled for the START pulse of the time-to-amplitude converter (TAC) at the different places. For the PEPICO mode, photoelectrons are utilized in the collision region, and for the PIPICO mode, photoions are used at the end of flight tube. The photoionization mass spectra were obtained at the PEPICO mode, and the PIPICO spectra were obtained by detecting ionic fragments in the PIPICO mode. Variation of the total PIPICO intensity with photon energy is obtained by recording PIPICO count rates and photon count rates simultaneously while the photon wavelength is scanned, and then by dividing the recorded PIPICO count rates by the recorded photon count rates. When we measured the PIPICO count rates, the coincidence time range (gate width in TAC) was set to be 0−10 μs, since the TOF difference between any pairs of ions formed from $SiBr_4$ falls in this time range.

In order to eliminate the unwanted higher order radiation energy in the range of 38−68 eV, a thin aluminum optical filter was employed. The slit width of the monochromator was 100 μm, giving an optical resolution of less than 0.1 and 0.2 nm at energies above and below 50 eV, respectively. The main chamber where the ionization cell and the TOF mass spectrometer were mounted was evacuated down to 1×10^{-8} Torr. When the $SiBr_4$ gas was introduced into the ionization cell, the pressure of the main chamber was maintained at about 6×10^{-7} Torr. The sample $SiBr_4$ with a nominal purity of 99+% was purchased from Aldrich Chemical Co. Inc. and used without further purification. No detectable impurities were observed in the TOF mass spectra.

The molecular geometry of $SiBr_4$ was optimized at the HF/6-31G* and MP2/6-31G* levels, with T_d symmetry. We also computed the term values corresponding to the Br(3d) core excitation, of $SiBr_3Kr^+$ at the HF/6-311++G* level at the experimental geometry of $SiBr_4$. All the calculations were carried out using a Gaussian 94 program suite[33] at SERI in Korea.

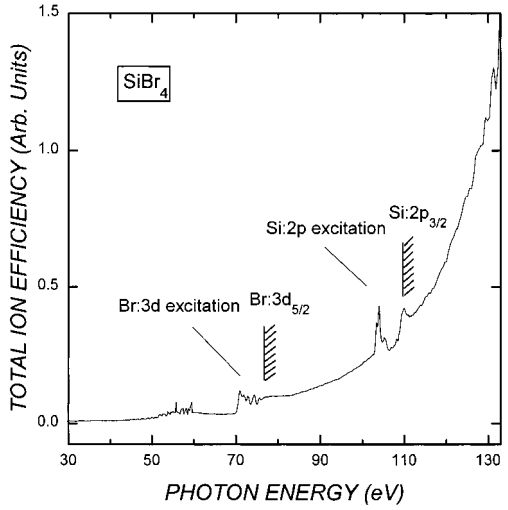

Figure 1. Total photoionization efficiency curve of $SiBr_4$ in the range 30−133 eV.

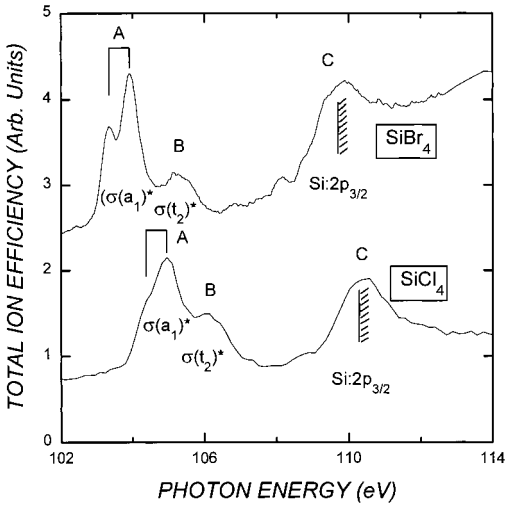

Figure 2. Total photoionization efficiency curve of $SiBr_4$ in the Si(2p) edge.

III. Results and Discussion

A. Photoionization Efficiencies. The total photoionization efficiency curve is presented in Figure 1. We have observed discrete resonances in the Br(3d) and Si(2p) regions over a structureless "giant resonance" beginning about 70 eV. The giant resonance peak never declines in the whole energy range examined.

(a) Si(2p) Excitation. Published experimental results on the photoabsorption and photoionization spectra of Si(2p) core level in SiX_4 (X = F,[7,11,14,20,21] Cl[4,19,22]) reveal that there are four group absorption bands in the range from 104 to 133 eV corresponding to the transition of the Si(2p) core electron to the $\sigma(a_1)^*$, $\sigma(t_2)^*$, e, and t_2 orbitals. The total photoionization efficiency curve in $SiBr_4$ in this range is similar to the photoionization spectrum of $SiCl_4$,[4,19] as shown in Figure 2. The peak positions of Si(2p) core electron excitation are also listed in Table 1 as well as those of SiX_4 (X = F, Cl) for comparison.

To assign the discrete excitations around the Si(2p) edge, we used the ab initio calculation result by Bodeur et al.[2] on the term values of PBr_4^+ which is a counterpart of the core-excited $SiBr_4$ in the view of the equivalent ionic core virtual orbital model (EICVOM),[14,34] although the Si(2p) electrons may not effectively screen the nuclear charge as in the case of the Si(1s) electrons. The binding energy of $Si(2p_{1/2})$ is estimated to be

TABLE 1: Peak Position in the Ion Yield Spectrum of SiX_4 (X = F, Cl, Br) in the Si(2p) Excitation

peak	energy, eV		
	$SiBr_4$	$SiCl_4$[a]	SiF_4[b]
A	103.9	105.0	106.5
B	105.3	106.1	108.5
C	109.9	110.6	117.0
D		121.4	130.0

[a] Reference 4. [b] Reference 20 and 21.

TABLE 2: Term Values (eV) of SiX_4 (X = Cl, Br) Determined by the HF and CI Calculation[a]

species	E_{TV}		E_{TV}	
	HF	CI	HF	CI
	$SiCl_4$		$SiBr_4$	
a_1	5.25	6.73	5.25	6.60
t_2	3.04	4.60	3.06	4.60
4s	2.31	2.48	2.31	2.49
4p	1.81	1.90	1.73	1.83
$3d_e$	1.33	1.35	1.28	1.31
$3d_{t_2}$	1.28	1.34	1.24	1.30
5s	1.21	1.26	1.16	1.22
5p	0.92	0.98	0.92	0.94

[a] Reference 2.

110.2 eV from the reported IP value for $Si(2p_{3/2})$ 109.6 eV,[35,36] and the spin−orbit splitting 0.6 eV.[11−13] Hence the excitation energy corresponding to $Si(2p_{1/2})$-to-$\sigma(a_1)^*$ can be estimated as 103.6 eV from the reported term value of 6.60 eV.[2] The value matches well with the experimental peak position of 103.9 eV as shown in Figure 2. For $SiCl_4$, the binding energy of $Si(2p_{1/2})$ is estimated to be 110.8 eV, the value obtained from the $Si(2p_{3/2})$ ionization limit of 110.18,[13] 110.17,[37,38] and 110.25 eV[36] and from the spin−orbit splitting 0.617 ± 0.005 eV in the spectra for SiX_4 (X = H, CH_3, F, Cl, etc.).[13] The excitation energy of 104.1 eV derived from the CI term value listed in Table 2 also closes to the observed excitation energy of 105.0 eV as seen in Figure 2.

Apparently, the peak A in Figure 2 consists of two maxima at 103.37 and 103.93 eV. The two peaks noted A originate from transitions of $Si(2p_{3/2}) \rightarrow \sigma(a_1)^*$ and $Si(2p_{1/2}) \rightarrow \sigma(a_1)^*$. There are three pieces of evidence supporting our assignment: (1) the peak shapes and splitting are quite similar to the photoabsorption spectra of SiX_4 (X = F, Cl); (2) the ab initio calculation indicates that there is a transition with a_1 symmetry occurring first in the Si(2p) excitation region; (3) the spin−orbit splitting of the Si(2p) electron was observed as 0.56 eV, in excellent agreement with the splitting value of 0.62 eV[11−13] for SiX_4 (X = F, Cl). However, the intensity ratio corresponding to $Si(2p_{3/2})$ and $Si(2p_{1/2})$, 1:1.4, considerably deviates from the statistical ratio of 2:1.[13]

For the transition of $Si(2p_{1/2})$ to $\sigma(t_2)^*$, we presume that peak B at 105.2 eV is a plausible candidate, since the transition is estimated to occur at about 105.2 eV, the energy predicted by the previous ab initio CI calculation.[2] The other peak corresponding to $Si(2p_{3/2}) \rightarrow \sigma(t_2)^*$ is most likely smeared in peak A. In the total photoionization efficiency curve of $SiCl_4$ (Figure 2), the peak corresponding to the same transition is on the shoulder of peak A.[4]

As discussed previously,[4] peak C seems to involve two or more transitions as seen in Figure 2 and more clearly in one of the insets in Figure 3 (PIPICO efficiency curve) and to involve $Si(2p_{1/2}) \rightarrow$ Rydberg (below the edge) and $Si(2p_{1/2}) \rightarrow$ e (shape resonance, above the edge).

In contrast to the case of SiF_4 and $SiCl_4$ at 130.0 and 121.4 eV, respectively, the shape resonance corresponding to the

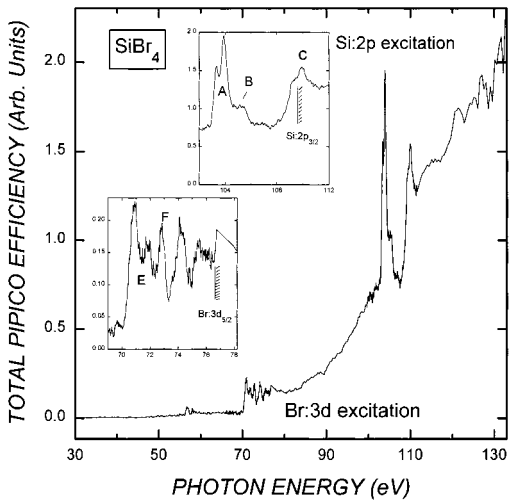

Figure 3. Total photoion−photoion coincidence efficiency curve of $SiBr_4$ in the range 30−133 eV. The insets show the scale-expanded spectra in the Si(2p) and Br(3d) excitation regions.

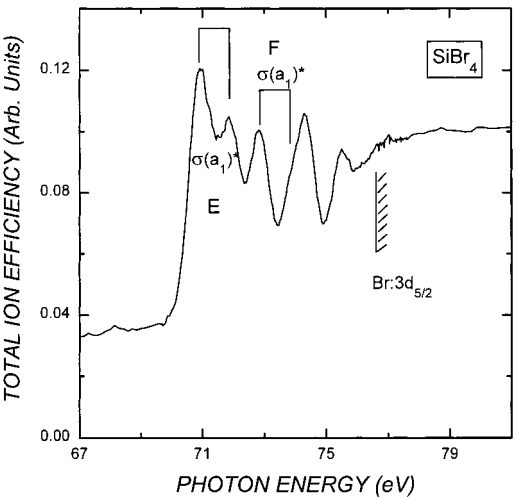

Figure 4. Total photoionization efficiency curve of $SiBr_4$ in the Br(3d) edge.

$Si(2p) \rightarrow t_2$ transition above the Si(2p) edge was apparently absent in Figure 1. We presume that the shape resonance is smeared in the giant resonance.

(b) Br(3d) Excitation. In the total photoionization efficiency curve of other silicon halides SiX_4 (X = F, Cl), a broad and structureless feature below 100 eV was observed, which is due to the valence single and double ionization via nonresonant processes.[4,11,19] In contrast to them, one group band is observed in the photoionization efficiency curve in $SiBr_4$ in the region of 70−80 eV (Figure 1). In Figure 4, we also present a scale-expanded spectrum to further elucidate the energetics and spectroscopy involved in the Br(3d) transition.

In order to assign the discrete transition observed in $SiBr_4$, we calculated the term values of the Br(3d)-to-valence and Br(3d)-to-Rydberg excited states. With the HF method using the 6-311++G* basis set, we carried out ab initio calculations on $SiBr_3Kr^+$, which is a counterpart of the Br(3d) core-excited $SiBr_4$ in the view of EICVOM. The first two peaks noted as E at 70.92 and 71.86 eV may correspond to the transition from the $Br(3d_{5/2})$ and $Br(3d_{3/2})$ orbitals to the a_1 antibonding orbital, respectively, the arguments based on the following observations and calculations. (1) The ab initio calculation showed that the $Br(3d) \rightarrow \sigma(a_1)^*$ transition occurs first in the range 70−80 eV. (2) The spectral splitting 0.94 eV may correspond to the spin−

TABLE 3: Term Values (eV) of $SiBr_3Kr^+$ Determined by the HF/6-311++G* Calculation at the Experimental Geometry of $SiBr_4$

species	E_{TV}
a_1	3.85
a_1	2.30
e	1.83
a_1	1.55
e	1.28
a_1	1.12
e	0.29
a_1	0.27
e	0.13

TABLE 4: Bond Lengths of Silicon Ligand

	Si−X bond length, Å	
molecule	calcd	exptl
$SiCl_4$	2.029 (HF/6-31G*) 2.028 (MP2/6-31G*)	2.019 ± 0.009[a]
$SiBr_4$	2.188 (HF/6-31G*) 2.193 (MP2/6-31G*)	2.17[b]

[a] Reference 39. [b] Extracted from ref 2.

orbit splitting of $Br(3d_{3/2,5/2})$, in excellent agreement with the reported value of 1.0 eV in BrCN molecule by Olney et al.[27]

The binding energy of $Br(3d_{5/2})$ of $SiBr_4$ is 76.6 ± 0.1 eV, the value averaged from the reported binding energies of 76.48 ± 0.05[35] and 76.64 ± 0.05 eV.[36] The excitation energy corresponding to the $Br(3d_{5/2}) \rightarrow \sigma(a_1)^*$ derived using the calculated term values listed in Table 3 is 72.7 eV, in fair agreement with the experiment value of 70.9 eV as shown in Figure 4. The values are predicted from the experimental geometry of $SiBr_4$. The discrepancy may reflect that the HF/6-311++G* calculation may greatly underestimate the term value and that the Br(3d) electrons cannot efficiently screen the nuclear charge owing to the extensive d character. It is noticed that as given in Table 2, the CI term values are generally in better agreement than the corresponding HF values.[2] Also the excitation energy 74.3 eV due to $Br(3d_{5/2}) \rightarrow \sigma(a_1)^*$ derived from the combination of theory and experiment is in fair agreement with the maximum value 72.8 eV of the peak F corresponding to $Br(3d_{5/2}) \rightarrow \sigma(a_1)^*$. Here it is also anticipated that the second a_1 term value (2.30 eV in Table 3) could be enhanced by the CI calculation on the equivalent core state. The calculations could provide information on the behaviors of the spectral splitting owing to a removal of the degeneracy arising from the transition of the Br core electron to the virtual valence orbital. It is noticed that the t_2 antibonding orbitals with T_d symmetry are broken into a_1 and e orbitals under C_{3v} symmetry.

B. Coincidence Spectra. *(a) PEPICO Spectra.* Figure 5 represents the mass spectra recorded at 30, 70, 75, 85, 104, 110, and 120 eV. The partial ion yields as a function of energy were derived on the basis of the mass spectra. Figure 6 shows variation of the ion yields with energy. The energy of 30 eV, the lowest energy examined, corresponds to valence ionization in which various monocations with the higher masses are formed. This is because, in the nonresonant processes, sufficient energy to break the Si−Br bonds cannot be left in the parent ion. In the excitation at about 75 eV, however, relatively sufficient energy could be stored in a molecule leading to the cleavage of the Si−Br bond. Owing to some local character of the Br(3d) orbitals, some excitation energy is stored in a specific Br atom rather than in the $SiBr_3^+$ counterpart. Thus the $SiBr_3^+$ ion is still cleanly observed, as shown in Figures 5 and 6.

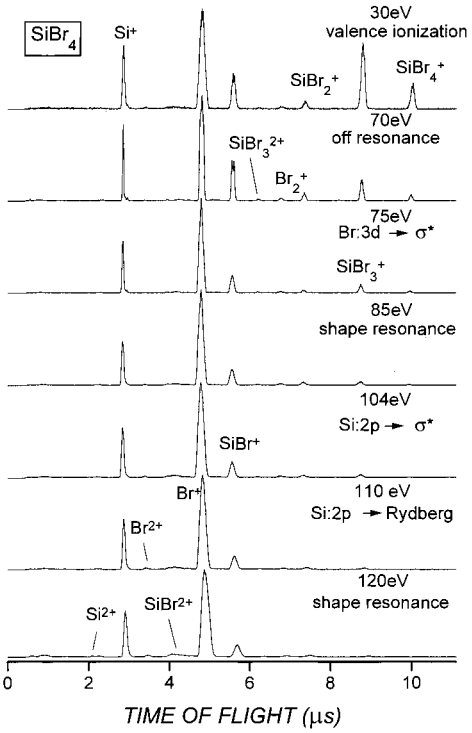

Figure 5. Photoelectron−photoion coincidence (mass) spectra of $SiBr_4$ measured at various photon energies.

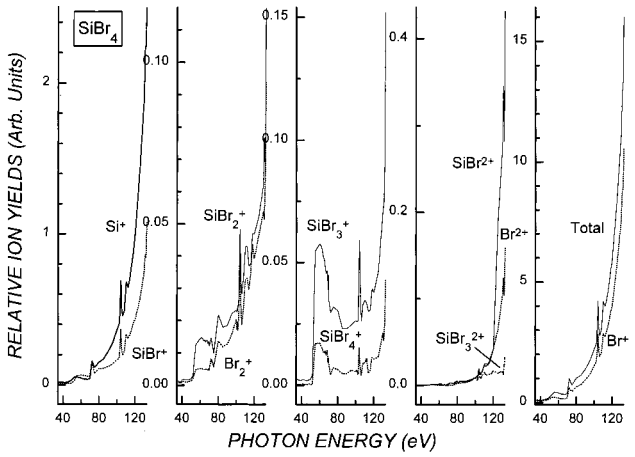

Figure 6. Partial photoion yield spectra of $SiBr_4$ in the range 30−133 eV. The spectral intensities ($I_{photoion}/I_{photon}$) are presented on the same relative intensity scale.

All the dications of Br^{2+} and $SiBr_n^{2+}$ (n = 1, 3) have significant yields when the energy reaches 120 eV. The ion yields increase with increasing the exciting photon energy. This trend has also been observed in the Si(2p) excitation of SiF_4[6,11] and $SiCl_4$[4] as well as the Br(3d) excitation of BrCN.[28] It is confirmed that the excitation of the Br(3d) core level electron leads to the various ionic dissociations of $SiBr_4$ rather than to the Coulomb explosion decomposition yielding bare Si^+ and its counterparts. In the Br(3d) transition, at least, one Br atom is more likely attached to the central Si atom until the ions reached the MCP detector. The previous studies on SiF_4[11] and $SiCl_4$[4] showed that changes in fragmentation and the total ion yields in passing from the valence region to the Si(2p) excitation regions were generally relatively small.

(b) PIPICO Spectra. In contrast to the total ion yield spectra, the PIPICO peaks are relatively sharp. This indicates that dissociative multiple ionizations are the main exit channel in the discrete resonance regions. In an attempt to elucidate the

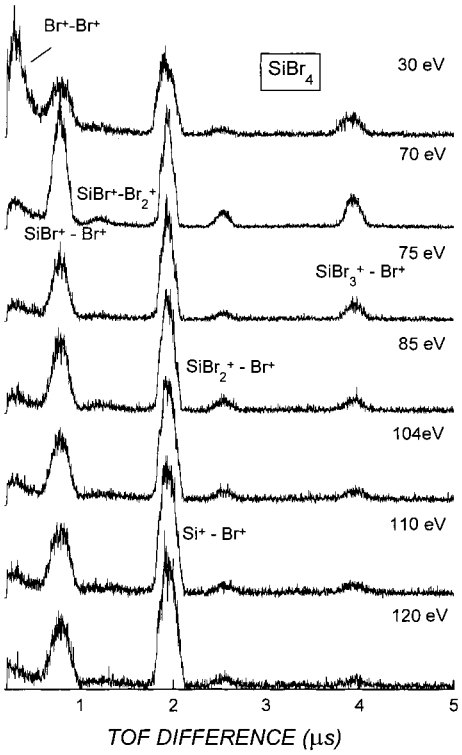

Figure 7. Photoion−photoion coincidence (PIPICO) spectra of $SiBr_4$ measured at various photon energies.

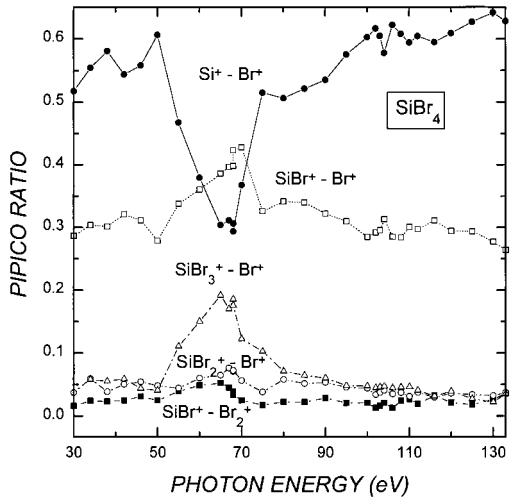

Figure 8. Ratios of integrated intensities of $SiBr_n^+-Br^+$ ($n = 0-3$) and $SiBr^+-Br_2^+$ ion pairs in PIPICO spectrum to total PIPICO ($I_{PIPICO}/I_{tot-PIPICO}$) in $SiBr_4$ as a function of photon energy.

major contributions of the total PIPICO yields, we present in Figure 7 typical spectra at some critical resonance energies and in some off-resonance regions. Processes leading to the ion pairs of $SiBr^+-Br^+$, $SiBr^+-Br_2^+$, Si^+-Br^+, $SiBr_2^+-Br^+$, and $SiBr_3^+-Br^+$ are observed in both of the excitation regions of both Br(3d) and Si(2p). Obviously, the ion pairs of Si^+-Br^+ and $SiBr^+-Br^+$ are most abundant in the whole energy range examined as seen in Figures 7−9. This observation is quite in contrast with those of SiF_4[11] and $SiCl_4$.[4] At low energies around 40 eV, $SiX_3^+-X^+$ (X = F, Cl) is the major PIPICO channel. For $SiBr_4$ at this energy, however, the $SiBr_3^+-Br^+$ channel is still minor.

In Figure 9, we present the individual PIPICO yield spectra in the range 30−133 eV. It is noticed that sum of the PIPICO yields for all the ion pairs is equal to the total PIPICO yield as

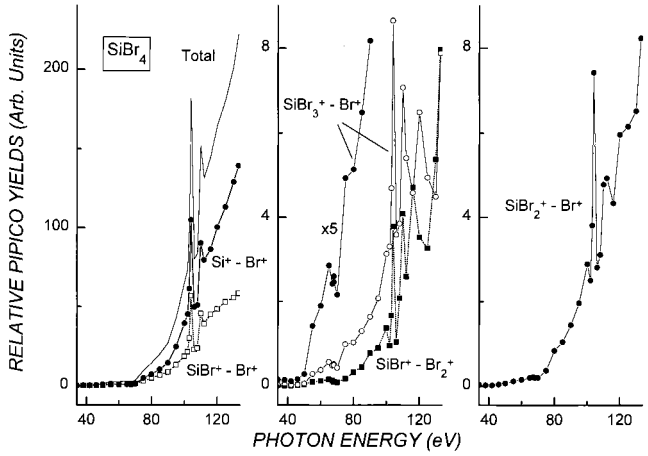

Figure 9. Photon energy dependence of the yields of the ion pairs detected by the PIPICO method. The spectral intensities (I_{PIPICO}/I_{photon}) are presented on the same relative intensity scale.

shown in Figure 3. The two prominent features seen in the SiF_4[11] and $SiCl_4$[4] PIPICO spectra have also been observed in the PIPICO spectra of $SiBr_4$ at about 104 and 110 eV. These energies correspond to the excitation of Si(2p) core electron to the $\sigma(a_1)^*$ and e orbitals (shape resonance), respectively.

Significant features in the PIPICO ratios are observed in the Br(3d) core excitation region (Figure 8). The sharp decline of the ion pair Si^+-Br^+, starting to rise at 50 eV, was compensated by the increase of ion pairs $SiBr^+-Br^+$ and $SiBr_3^+-Br^+$. Comparing the PIPICO yield and PIPICO ratio in $SiBr_4$ with our previous results of $SiCl_4$,[4] it is found that the most intense ion pair is Si^+-Br^+ except in the Br(3d) region, whereas in $SiCl_4$, the signal corresponding to $SiCl^+-Cl^+$ is most intense.

C. Dissociation Pattern. A hole in the Si(2p) orbital resulting from the excitation of an Si(2p) electron will electronically relax before $SiBr_4$ begins to fragment. Such dominant relaxation processes are expected to occur via the double-resonant Auger processes, which can involve the ejection of two or more electrons.[5,11] When an Si(2p) core electron is initially excited to a virtual orbital (1 hole and 1 excited electron), $SiBr_4$ will be left as a doubly charged ion. Various ion pairs are expected to be formed from the Coulomb explosion of such doubly charged precursor ion or fragment ions, because in polyatomic molecules in general, there are several possible combinations of valence MO's in which two holes are produced.

It is shown in the Si(2p) region that the PIPICO channels shown in reactions 1 and 2 may account for 90 ± 1% of the whole PIPICO signals.

$$SiBr_4 + h\nu \rightarrow Si^+ + Br^+ + np + 2e \quad (1)$$

$$SiBr_4 + h\nu \rightarrow SiBr^+ + Br^+ + np + 2e \quad (2)$$

np denotes neutral product(s). However, it is elucidated that such simple Coulomb explosion cannot explain the formation of the Br^+ ion with 68% in the total ion intensity at 110 eV.

It is useful to notify that our simple PIPICO method may not clarify the occurrence of triple photoionization, but the method may hint its possibility by comparing the ion intensity ratios as a function of energy. In Figure 11, we present the variation of the ratio of the ion intensity for Br^+ to sum of the intensities for $SiBr_n^+$ ($n = 0-3$) with the photon energy. For example, in the case that only the double ionization followed by processes 1 and 2 occurs, the ratio should become 1. In the Br(3d) excitation region, we presume that reactions 1−3 would

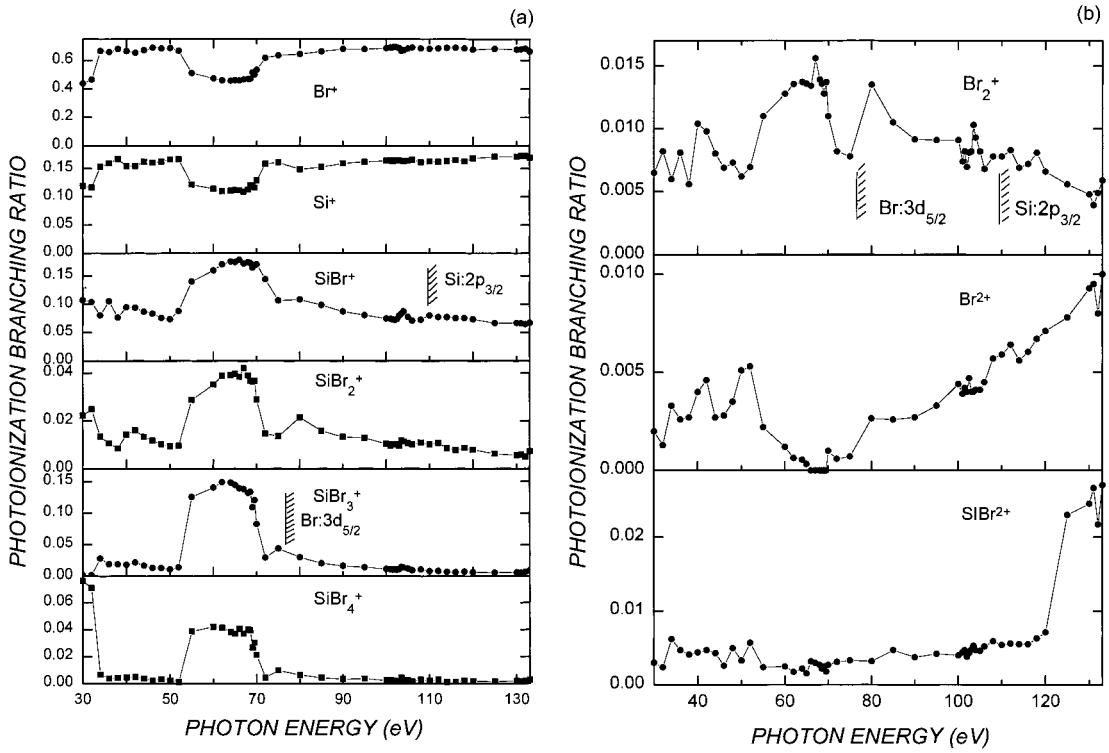

Figure 10. Ratios of integrated intensities of ion peaks in the TOF mass spectra to total photoion intensity ($I_{photoion}/I_{tot-photoion}$) in $SiBr_4$ as a function of photon energy.

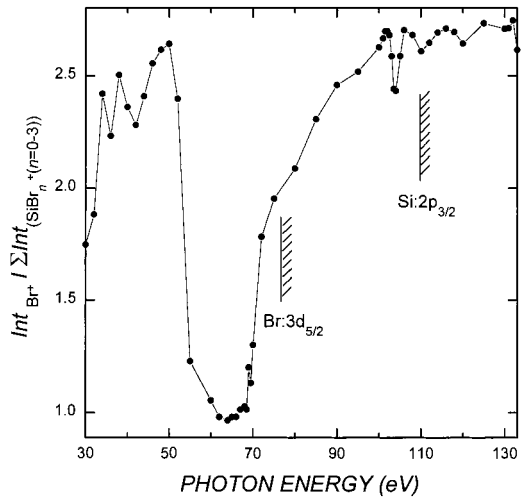

Figure 11. Ratios of integrated intensities of Br^+ in the TOF spectra to sum of intensities of $SiBr_n^+$ ($n = 0-3$) in $SiBr_4$ as a function of photon energy.

occur dominantly, since the ratio is about 1 (Figure 11).

$$SiBr_4 + h\nu \rightarrow SiBr_3^+ + Br^+ + 2e \qquad (3)$$

In the other valence and core excitation reions, the ratio is larger than 2, indicating that the multiple ionization followed by several dissociation processes, for example, reactions 4 and 5, would prevail.

$$SiBr_4 + h\nu \rightarrow Si^+ + 2Br^+ + Br + 3e \qquad (4)$$

$$SiBr_4 + h\nu \rightarrow SiBr^+ + 2Br^+ + Br + 3e \qquad (5)$$

It seems odd that the Br^+-Br^+ channel is observed dominantly (Figure 7) in the valence excitation/ionization region. This observation can support than the ratio is larger than 2. However, the fundamental source for this behavior is unknown.

IV. Conclusions

The present coincidence spectroscopic study led to the detection of various monocations of Br_n^+ ($n = 1, 2$) and $SiBr_n^+$ ($n = 0-4$) along with dications of Br^{2+} and $SiBr_n^{2+}$ ($n = 0, 1, 3$) in the whole energy range 30−133 eV. Among the ions, Si^+, Br^+, and $SiBr^+$ are predominantly observed in the whole range, both in the nonresonant ionization and in the core to valence/Rydberg excitation regions. In the photoionization efficiency and PIPICO curves, we have observed the prominent features in the Si(2p) and Br(3d) edges owing to their enhanced oscillator strengths. We have assigned the discrete resonance energies of $SiBr_4$ below the Si(2p) and Br(3d) ionization edges by using the equivalent ionic core approximation method and then by performing the HF/6-311++G* calculation on $SiBr_3$-Kr^+. In contrast to the Si(2p) core excitation, the Br(3d) core excitation led to the detection of ion pair $SiBr_3^+-Br^+$ with significant yields. This implies that the excitation of one of the Br core weakens the specific Si−Br bond in the energy dissipation processes.

Acknowledgment. This work was partially supported by the Korea Research Foundation as an international collaborative research project (1996−1997). We are grateful to Prof. K. Mitsuke at IMS for his beam time arrangement and helpful discussion, and to Mr. E. Nakamura (IMS) for his great help in conducting this experiment. The members of the UVSOR facility at Institute for Molecular Science in Okazaki, Japan, are greatly acknowledged for their valuable help.

References and Notes

(1) Bodeur, S.; Millie, P.; Lugrin, E. L.; Nenner, I.; Filipponi, A.; Boscherini, F.; Mobilio, S. *Phys. Rev. A* **1989**, *39*, 5075.

(2) Bodeur, S.; Millie, P.; Nenner, I. *Phys. Rev. A* **1990**, *41*, 252.

(3) Sutherland, D. G. J.; Kasrai, M.; Bancroft, G. M.; Liu, Z. F.; Tan, K. H. *Phys. Rev. B* **1993**, *48*, 14989.
(4) Boo, B. H.; Park, S. M.; Koyano, I. *J. Phys. Chem.* **1995**, *99*, 13362.
(5) Boo, B. H.; Lee, S. Y.; Kim, H.; Koyano, I. *J. Phys. Chem.* **1996**, *100*, 523.
(6) Lablanquie, P.; Souza, A. C. A.; de Souza, G. G. B.; Morin, P.; Nenner, I. *J. Chem. Phys.* **1989**, *90*, 7078.
(7) de Souza, G. G. B.; Morin, P.; Nenner, I. *J. Chem. Phys.* **1989**, *90*, 7071.
(8) Bozek, J. D.; Tan, K. H.; Bancroft, G. M.; Fu, K. *J. Chem. Phys.* **1991**, *158*, 171.
(9) Winkler, D. C.; Moore, J. H.; Tossell, J. A. *Chem. Phys. Lett.* **1994**, *222*, 1.
(10) Nagaoka, S.; Ohshita, J.; Ishikawa, M.; Takano, K.; Nagashima, U.; Takeuchi, T.; Koyano, I. *J. Chem. Phys.* **1995**, *102*, 6078.
(11) Imamura, T.; Brion, C. E.; Koyano, I.; Ibuki, T.; Masuoka, T. *J. Chem. Phys.* **1991**, *94*, 4936.
(12) Sutherland, D. G. J.; Bancroft, G. M.; Tan, K. H. *J. Chem. Phys.* **1992**, *97*, 7918.
(13) Bozek, J. D.; Bancroft, G. M.; Tan, K. H. *Phys. Rev. A* **1991**, *43*, 3597.
(14) Friedrich, H.; Pittel, B.; Rabe, P.; Schwarz, W. H. E.; Sonntag, B. *J. Phys. B: Atom. Mol. Phys.* **1980**, *13*, 25.
(15) Simon, M.; Lebrun, T.; Martins, R.; de Souza, G. G. B.; Nenner, I.; Lavollee, M.; Morin, P. *J. Phys. Chem.* **1993**, *97*, 5228.
(16) Ishikawa, H.; Fujima, K.; Adachi, H.; Miyauchi, E.; Fujii, T. *J. Chem. Phys.* **1991**, *94*, 6740, and refs therein.
(17) Tse, J. S.; Liu, Z. F.; Bozek, J. D.; Bancroft, G. M. *Phys. Rev. A* **1989**, *39*, 1791.
(18) Sodhi, R. N. S.; Daviel, S.; Brion, C. E.; de Souza, G. G. B. *J. Electron Spectrosc. Relat. Phenom.* **1985**, *35*, 45.
(19) Boo, B. H.; Park, S. M.; Koyano, I. *J. Korean Phys. Soc.* **1998**, *32*, 513.
(20) Vinogradov, A. S.; Zimkina, T. M. *Opt. Spectrosc. (USSR)* **1971**, *31*, 288.
(21) Zimkina, T. M.; Vinogradov, A. S. *J. Phys. (Paris) Colloq.* **1971**, *32*, C4-3.
(22) Nagaoka, S.; Ohshita, J.; Ishikawa, M.; Masuoka, T.; Koyano, I. *J. Phys. Chem.* **1993**, *97*, 1488.
(23) Streubel, P.; Franke, R.; Chasse, T.; Fellenberg, R.; Szargan, R. *J. Electron Spectrosc. Relat. Phenom.* **1991**, *57*, 1.
(24) Mazzoni, M.; Pettini, M. *Phys. Lett.* **1981**, *A85*, 331.
(25) Nahon, L.; Morin, P.; Combet-Farnoux, F. *Phys. Scr.* **1992**, *41T*, 104.
(26) Cummings, A.; O'Sullivan, G. *Phys. Rev. A* **1996**, *54*, 323 and refs therein.
(27) Olney, T. N.; Brion, C. E.; Ibuki, T. *Chem. Phys.* **1995**, *201*, 505.
(28) Ibuki, T.; Hiraya, A.; Olney, T. N.; Brion, C. E. *Chem. Phys.* **1996**, *203*, 359.
(29) Masuoka, T.; Horigome, T.; Koyano, I. *Rev. Sci. Instrum.* **1989**, *60*, 2179.
(30) Ishiguro, E.; Suzui, Yamazaki, J.: M.; Nakamura, E.; Sakai, K.; Matsudo, O.; Mizutani, N.; Fukui, K.; Watanabe, M. *Rev. Sci. Instrum.* **1989**, *60*, 2105.
(31) Masuoka, T.; Koyano, I. *J. Chem. Phys.* **1991**, *95*, 909.
(32) Masuoka, T.; Koyano, I.; Saito, N. *Phys. Rev. A* **1991**, *44*, 4309. *115*, 157.
(33) Frisch, M. J.; Trucks, G. W.; Schlegel, H. B.; Gill, P. M. W.; Johnson, B. G.; Robb, M. A.; Cheeseman, J. R.; Keith, T.; Petersson, G. A.; Montgomery, J. A.; Raghavachari, K.; Al-Laham, M. A.; Zakrzewski, V. G.; Ortiz, J. V.; Foresman, J. B.; Cioslowski, J.; Stefanov, B. B.; Nanayakkara, A.; Challacombe, M.; Peng, C. Y.; Ayala, P. Y.; Chen, W.; Wong, M. W.; Andres, J. L.; Replogle, E. S.; Gomperts, R.; Martin, R. L.; Fox, D. J.; Binkley, J. S.; Defrees, D. J.; Baker, J.; Stewart, J. P.; Head-Gordon, M.; Gonzalez, C.; Pople, J. A. *Gaussian 94*, Revision D.2; Gaussian, Inc: Pittsburgh, PA, 1995.
(34) Schwarz, W. H. E.; Buenker, R. J. *Chem. Phys.* **1976**, *13*, 153.
(35) Drake, J. E.; Riddle, C.; Henderson, H. E.; Glavincevski, B. *Can. J. Chem.* **1976**, *54*, 3876.
(36) Perry, W. B.; Jolly, W. L. *Inorg. Chem.* **1974**, *13*, 1211.
(37) Kelfve, P.; Blomster, B.; Siegbahn, H.; Siegbahn, K.; Sanhueza, E.; Goscinski, O. *Phys. Scr.* **1980**, *21*, 75. *203*, 359.
(38) Drake, J. E.; Riddle, C.; Coatsworth, L. *Can. J. Chem.* **1975**, *53*, 3602.
(39) Ryan, R. R.; Hedberg, K. J. *J. Chem. Phys.* **1969**, *50*, 4986.